Single Screw Extrusion Compounding of Particulate Filled Thermoplastics: State of Dispersion and Its Influence on Impact Properties

YEH WANG* and JIANG-SHEN HUANG

Department of Chemical Engineering, P.O. Box 833, Tunghai University, Taichung, Taiwan 407, Republic of China

SYNOPSIS

The compounding of calcium carbonate filled polypropylene (PP) is discussed with reference to a single-screw extruder and variants of mixing sections. The mixing section on the screw is exchangeable, and two dispersive mixing elements, namely the Zorro and the Maddock elements, were used. The calcium carbonate was surface treated with a liquid titanate coupling agent (LICA12). The impact strength was measured by a notched Izod impact tester with specimens having a U-shaped sharp notch. The fracture toughness for the PP homopolymer and the filled composites was determined using fracture mechanics principles. The results were correlated with the state of dispersion of the calcium carbonate filler. The effects of filler concentration and surface treatment were examined as well. Correlation between state of dispersion and impact properties for calcium carbonate filled PP was obtained. We also investigated the effect of various mixing elements on the state of dispersion. The experimental results indicate that good dispersion would improve the impact properties of the polymer matrix, but only at moderate filler loading. © 1996 John Wiley & Sons, Inc.

INTRODUCTION

Single-screw extruders are commonly encountered in polymer applications. A major task of these machines is polymer compounding, for example, the melt blending of thermoplastics and the incorporation of fibrous and particulate additives to modify physical properties. Even though twin-screw extruders have dominated the compounding industries in recent years, single-screw extruders still have a significant market share due to their low cost and easy maintenance.

It has been a widespread practice to incorporate mineral fillers into thermoplastics to extend them and to enhance certain properties. The degree of improvement depends on the judicious choice of filler origin, particle size and shape, fraction of filler.[1-7] and surface treatment to modify interaction between the polymer matrix and filler.[8-12] To optimize the properties of filled compounds, however, effective mixing is also of paramount importance to achieve adequate spatial distribution and dispersion of filler particles.[13-15] The mixing efficiency is often limited in a single-screw extruder because of the nonuniform shear strain history and melt temperature distribution generally occurring in such machines.[16] A variety of mixing elements have been produced for single-screw extruders in order to improve different mixing tasks. The question then becomes, what mixing elements have the ability to achieve a high degree of filler dispersion in a polymer matrix? Thus characterization of dispersion becomes important in this respect.

Various techniques have been reported for the determination of dispersion. The dispersion state of small particle filled elastomers has been characterized by optical microscopy,[17-19] electron microscopy,[20,21] surface roughness,[22] electrical conductivity,[20,23] and small angle light scattering.[24] More recently the microscopy method[25] and small light

* To whom correspondence should be addressed.

Journal of Applied Polymer Science, Vol. 60, 1779–1791 (1996)
© 1996 John Wiley & Sons, Inc. CCC 0021-8995/96/111779-13

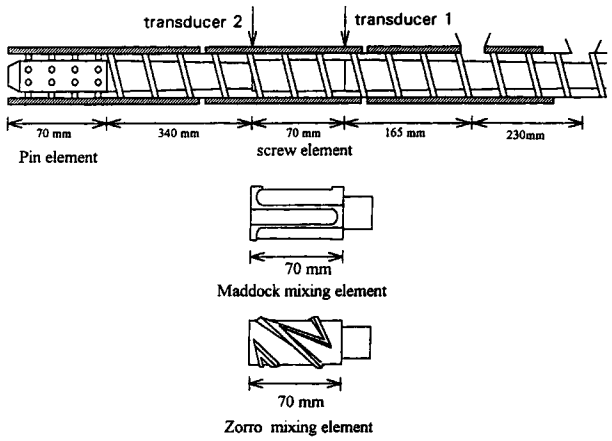

Figure 1 Schematics of screw configuration and various mixing elements.

scattering technique[26] have been applied to particulate-filled thermoplastics. Recent advances in computerized image analysis have promoted several studies relating to the characterization of dispersion in mineral-filled thermoplastics. Ess et al.[13] numerically quantified agglomerate levels in polypropylene (PP) compounds containing 40 wt % $CaCO_3$ based on the analysis of scanning electron microscopy (SEM) images. Suetsugu et al.[27] applied a similar technique to examine the effect of processing conditions on PP systems containing 20 wt % $CaCO_3$.

To control and improve the mechanical properties of the particulate-filled polymeric materials, it is desirable to understand the relations between processing, structure, and properties. In the present work, we characterized the structure of composites in terms of the state of dispersion of the filler through the use of SEM in conjunction with a commercial image analysis system. Special attention was paid to the investigation of large aggregates and agglomerates existing in the materials. Two dispersive mixing elements, namely the Zorro and the Maddock elements, were used for compounding in a single-screw extruder. As a comparison to these mixing elements, an ordinary screw element was also used. The calcium carbonate filled PP was used as a model compound. Dispersion degree represented by the area fraction of agglomerates of filler was quantitatively determined. Notched Izod impact properties were analyzed as a function of the dispersion degree using fracture mechanics principles. The failure mechanism and the effects of filler concentration and surface treatment were investigated as well.

EXPERIMENTAL

Materials

General purpose isotactic PP (i-PP) homopolymer (Yungsox 1040) provided by the Yung-Chia Chemical Co., Taiwan, was used in this study. The density of the PP was 904 kg/m^3 measured with an electronic densimeter. The calcium carbonate, trade name Hydrocarb 900G, was supplied from Omya, Switzerland. Its average particle size was 0.8 μm and the specific gravity was 2.7. Both quantities were reported by the manufacturer. The surface treatment was carried out by Taiwan Huntsman Co. with 0.3 wt % LICA12 (Kenrich Petrochemicals Inc., USA). LICA12 is a liquid titanate coupling agent that is well known for its effective modification of the inorganic filler surface.[7,28,29] To all the compounds, 0.2 wt % heat stablizer (EVERNOX-10, Everspring Chemical Co., Taiwan) was added to prevent degradation of the polymer during compounding. PP and the stabilizer were dry blended at room temperature after dehumidifying.

Compounding Procedures

The polymer pellets and mineral additive were metered independently in the required proportions using volumetric dosing units. The pellets were fed into the throat of the extruder, and the mineral powder was introduced separately through a downstream feeding port into the partially melted polymer. It was found that if the pellets and the additive were premixed and fed into the primary feed port together, the final compounds were extremely inhomogeneous. However, if the polymer was in powder form, then the premix was an efficient way for compounding.[13] Compounding was carried out on a single-screw extruder with a diameter of 35 mm and an L/D ratio of 26 (Tungtai Machine Co., Taiwan) over a modular mixing section and well-defined processing conditions. The melt was extruded through a 20-mm wide and 3-mm thick sheeting die, and was

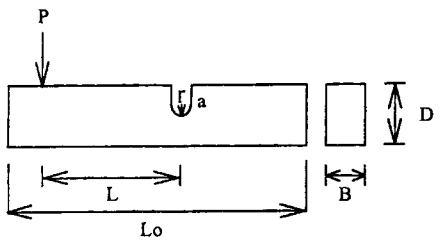

Figure 2 Dimension of specimen for Izod impact test.

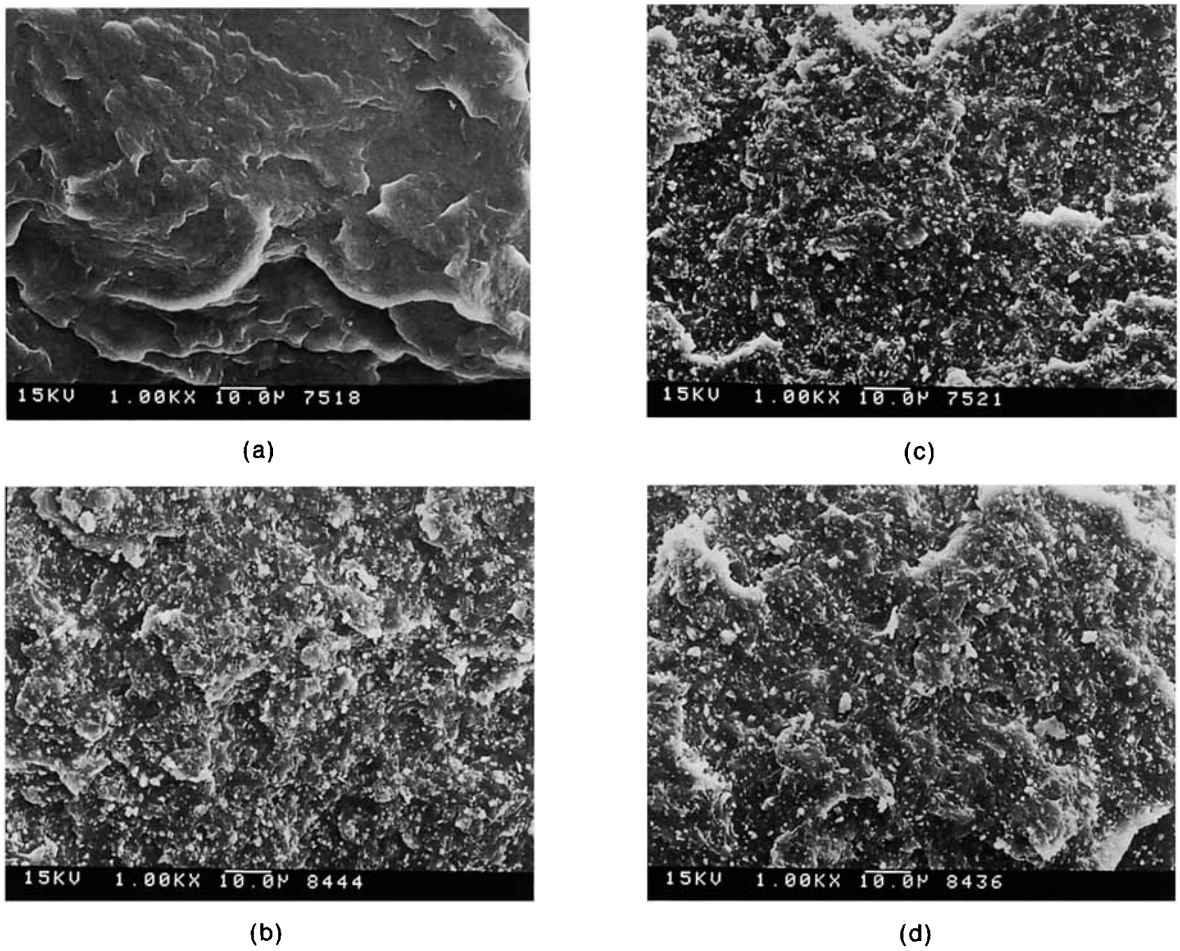

Figure 3 Scanning electron micrographs of composites filled with untreated $CaCO_3$: (a) fracture surface of pure polypropylene, (b) fracture surface of the composite from the Maddock element, (c) fracture surface of the composite from the Zorro element, and (d) fracture surface of the composite from the screw element. Filler concentration is 12 vol %.

collected as an unsized strip with two sets of take-up rolls. The temperature of the front roll was controlled by the heating oil from a constant temperature oil bath. The oil temperature was set at 30°C for all experiments. Filler concentrations of 20, 12, and 5 vol % (43, 29, and 14 wt %) were compounded.

Screw Configurations

The mixing section of the single screw has a provision for complete interchangeability. In this work the effect on dispersive mixing of altering mixing sections was considered. In the standard screw configuration, the first stage of the machine delivers polymer from the feed hopper through the heating zone. This section is immediately followed by the second feed port. The mixing section is next to the second feed port. The remaining part of the screw, which is the metering section, further mixes, conveys, and pressurizes material prior to passage through the die adaptor and then the sheeting die. An additional pin mixing element (distributive type) was located at the screw head. Such arrangement is standard in the dispersive mixing practice. The schematics of the complete screw and the mixing elements are shown in Figure 1.

Processing Variables

In addition to the screw configuration, the principal process variables considered were screw speed and barrel temperature profiles. After several trials, the screw speed was set at 45 rpm, and the barrel temperature profiles were set at 180°C in the first zone (feed section), 180°C in the second zone (mixing section), 185°C in the third zone

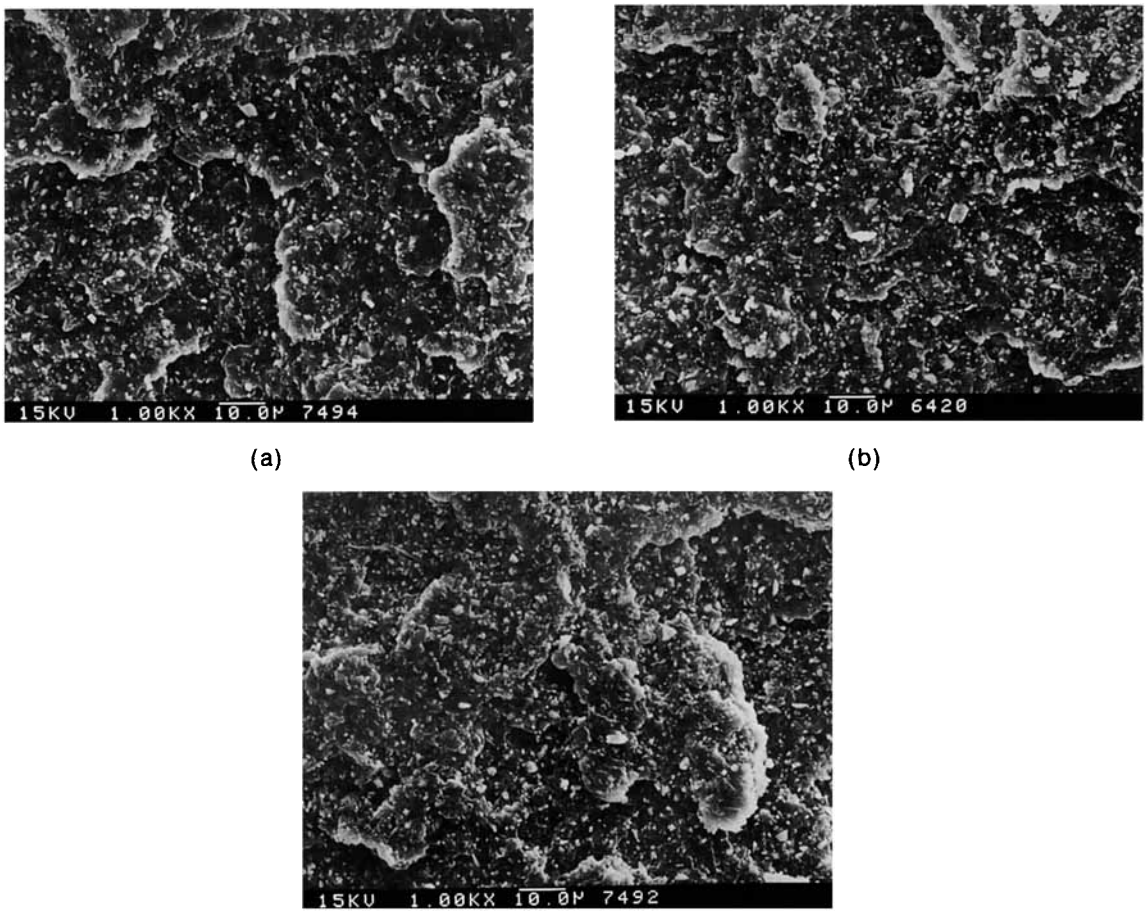

Figure 4 Scanning electron micrographs of composites filled with LICA12 treated $CaCO_3$: (a) fracture surface of the composite from the Maddock element, (b) fracture surface of the composite from the Zorro element, and (c) fracture surface of the composite from the screw element. Filler concentration is 12 vol %.

(metering section), 190°C in the die adapter, and 195°C in the sheeting die. The speed and the temperatures were fixed for all experiments. A further variable, generally encountered in a metered-fed extruder, is the feed rate. For each formulation, throughput was maximized to an upper limit such that flooding from the secondary port could be avoided. The feed rate was within the range of 1.7–2.5 kg/h.

Characterization of Dispersion

The microscopy work was done with SEM on a TOPCON ABT-150S using a secondary detector. The fracture surfaces of specimens from impact testing used for fractographic analysis were gold coated in a sputtering chamber prior to SEM studies. The acceleration voltage used was 15 kV. The SEM micrographs were then digitized by an electronic scanner (TG400 National CCD camera). The digitized grey level images represent a resolution of 480 × 640 pixels. The images were quantified using a 386-based personal computer equipped with an Optimas 4.0 image processing system from Bioscan USA. Optimal delineation between the polymer matrix and the dispersed phase particles and agglomerates was determined empirically by adjusting the grey level of the image. This was set at 240 on a 0 (black) to 256 (white) scale and was held constant throughout. Particle domains were characterized by counting the number of pixels, with brightness levels falling within the designated grey scale range of 240–256. Equivalent spherical diameters were computed based on

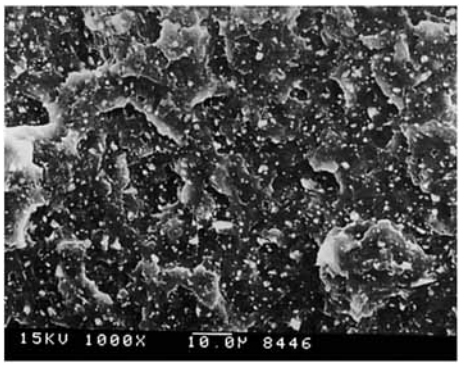

(a)

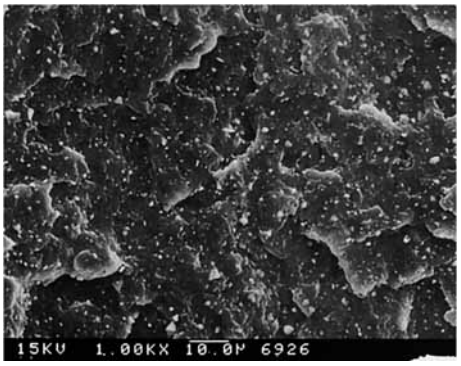

(b)

Figure 5 Scanning electron micrographs of composites from the Maddock element: (a) fracture surface of the composite filled with untreated $CaCO_3$ and (b) fracture surface of the composite filled with LICA12 treated $CaCO_3$. Filler concentration is 5 vol %.

the illuminated pixel regions. Size and area data was then inventoried and classified.

Notched Izod Impact Test

Test pieces for impact testing were compression molded from the extruded sheets under pressure at 200°C for 30 min before slow cooling. The notched Izod test specimens followed the ASTM D256 norms; detailed dimensions of the specimen and the notch are shown in Figure 2. All test pieces were given a U-shaped sharp notch with a tip radius of about 0.085 mm using a diamond cutter. The initial crack depth varied from $a = 1$ to 3 mm. The notched samples were used for studying the impact properties with an Izod impact tester at a room temperature of around 18°C. At least six specimens were tested for each compound. Fracture surfaces were also studied with the aid of SEM to understand the mechanism of failure.

RESULTS AND DISCUSSION

Fractography

The SEM micrographs of the fractured surfaces of the neat polymer and the i-PP/$CaCO_3$ composites from impact testing are presented in Figure 3(a–d). The brittle behavior of the matrices at room temperature was confirmed by the observed morphology of the fracture surface of the virgin PP [Fig. 3(a)] similar to published reports.[27,30,31] The fracture surfaces of the untreated $CaCO_3$ filled composites compounded from the Zorro element, the Maddock element, and the screw element are presented in Figure 3(b–d). The filler concentrations are 12% by volume. The presence of particles several microns in size could be observed in these composites. Although it seems that more large particles and agglomerates are present in the composites compounded from the screw element, these specimens generally show poor dispersion in the iPP matrix, regardless of the type

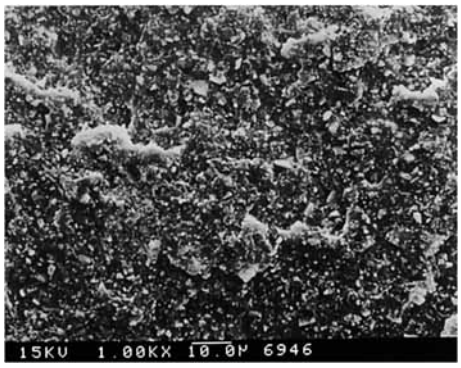

(a)

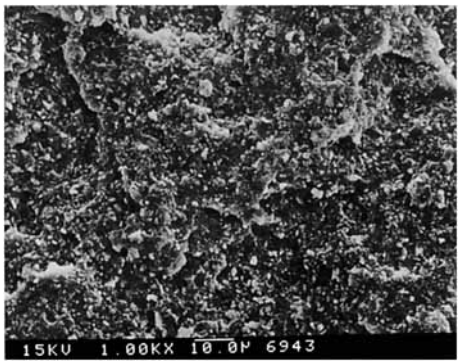

(b)

Figure 6 Scanning electron micrographs of composites from the Maddock element: (a) fracture surface of the composite filled with untreated $CaCO_3$ and (b) fracture surface of the composite filled with LICA12 treated $CaCO_3$. Filler concentration is 20 vol %.

of mixing elements used in compounding. Such poor dispersion may be ascribed to the crystalline nature of the polymer and the agglomeration tendency of the fine $CaCO_3$ particles.[29,32] The filler particles agglomerate to larger shapes and only a limited quantity of polymer residue adheres to the filler surface. Similar to the virgin PP, the fracture surfaces appear to be nonuniform with random fracture and uneven voids, which may indicate a low degree of deformation and a large amount of voids in the specimens. The observed crack spread mainly through the weakest track in the composite. Hence, the fracture proceeded along the PP–$CaCO_3$ interface so that abundent $CaCO_3$ particles can be observed on the fracture surfaces. It seems that some of the $CaCO_3$ particles popped out of the polymer matrix, even though the dewetting stress is usually high around the untreated $CaCO_3$ particles.[33]

The fracture surfaces of the specimens filled with LICA12 treated $CaCO_3$ compounded from the Zorro element, the Maddock element, and the screw element are presented in Figure 4(a–c). The filler concentrations are also 12% by volume. It can be clearly seen that there are fewer large particles or agglomerates in these composites when compared with the micrographs of untreated $CaCO_3$ shown in Figure 3(b–d). As expected, there are also more large particles and agglomerates in the composites compounded from the screw element. In general, better dispersion with a low degree of agglomeration of the filler was observed with surface treated $CaCO_3$ filled compounds. Phase separation between the filler particles and the matrix seems less distinct due to effective modification of the filler surface with LICA12, resulting in fewer agglomerated particles present on the fracture surface.

The fracture surfaces of the specimens compounded from the Maddock element with untreated and surface treated $CaCO_3$ at 5 vol % are presented in Figure 5(a,b). While it seems that fewer particles are seen on the fracture surfaces than that at 12 vol %, the number of agglomerates and large particles is not reduced much. Unlike the case at 12 vol %, the surface treatment seems to not affect the filler dispersion very much at such low filler concentration when comparing Figure 5(a) with 5(b).

The fracture surfaces of the specimens compounded from the Maddock element with untreated and surface treated $CaCO_3$ at 20 vol % are presented in Figure 6(a,b), respectively. A large amount of the agglomerated particles and structural inhomogeneities can be seen in both SEM micrographs. We think such inefficient mixing observed at 20 vol % is because the size of the lab screw used in these experiments may be so small that the adjustable operation factors such as feed rate or screw speed are too limited to effectively incorporate fillers of such high concentration into the polymer matrix. However, with a large diameter screw and wider operation range, the compounding at high filler concentration should be improved.

Determination of Dispersion Degree

Dispersion degree was characterized by measuring the size and the number of agglomerates. Agglomerates may act as defects in the composites because of their large size and relatively weak structure formed by interparticle forces. Dispersion degree may be defined as a function of area fraction, Φ_a, of agglomerates.

$$\Phi_a = \sum \pi d_i^2 n_i / 4A \qquad (1)$$

where A is the area of observation, d_i is the diameter of the agglomerates, and n_i is the number of agglomerates. Large value of Φ_a indicates poor dispersion of fillers. Other higher order averages may also be considered. However, it has been found that the mechanical properties correlated well with the area fraction of the agglomerates.[27,34]

The particle size distributions of untreated $CaCO_3$ at 12 vol % from the Zorro, the Maddock, and the screw elements are shown in Figure 7(a). While there is not much difference in the shape of these curves, the peak around 0.6 μm, which is about the size of a unit particle or aggregate, is much lower for the screw element; and the peak heights do not differ much for the two dispersive elements. Furthermore, the long tail in each curve indicates the existence of agglomerates and large particles. The calculated mean particle sizes are listed in Table I. The mean size is also the largest in the composites from the screw element; and it is even bigger than the original size before compounding. Moreover, the mean sizes for the two dispersive elements are only slightly smaller than the original size.

The particle size distributions of treated $CaCO_3$ at 12 vol % from the Zorro, the Maddock, and the screw elements are shown in Figure 7(b). Similarly, a peak around 0.6 μm is shown in all three curves and a long tail can also be seen. The peak height is also the lowest for the screw element. The calculated mean particle sizes are listed in Table I. That the mean sizes of treated $CaCO_3$ are all smaller than their untreated counterparts demonstrates LICA12's ability as an effective coupling agent. The mean size

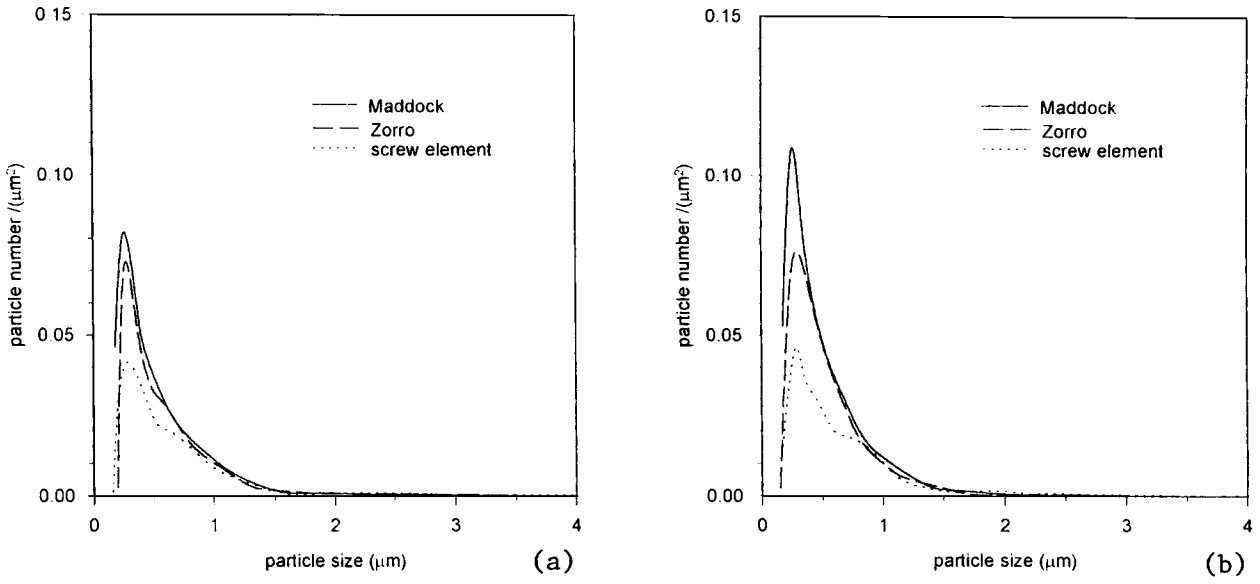

Figure 7 Particle size distribution of $CaCO_3$ filled composites from various mixing elements at 12 vol %: (a) without surface treatment and (b) with surface treatment.

is still the largest in the composites from the screw element. The differences between the mean sizes for the two dispersive elements and the original size, however, become more significant than the untreated fillers.

The particle size distributions of untreated and LICA12 treated $CaCO_3$ filled composites at 5 vol % from the three elements are shown in Figure 8(a,b). The shapes of these distribution curves are similar to that shown in Figure 7(a,b) at 12 vol %. One single peak around 0.6 μm and a long tail can be clearly seen for each curve. However, the peak heights are much lower than in Figure 7(a,b). This was expected because the fraction of the unit particles and aggregates in the composites will be less when the filler concentration becomes lower. The calculated mean particle sizes at 5 vol % are also listed in Table I. These mean sizes are all smaller than their counterparts at 12 vol % due to less agglomeration of particles at low filler concentrations. The mean particle sizes at 20 vol % from the Maddock element are also included for comparison. They are the largest among all the samples under consideration.

Table I Calculated Mean Particle Size from Specimens Compounded from Various Mixing Elements

Surface Treatment	Maddock	Zorro	Screw Element
Without			
5 vol %	0.7248	0.7485	0.7839
12 vol %	0.7384	0.7537	0.8465
20 vol %	0.9151		
With			
5 vol %	0.6847	0.7135	0.7467
12 vol %	0.6943	0.7264	0.8227
20 vol %	0.9094		

Values in microns.

The distribution curves of the area fraction of untreated $CaCO_3$ filled composites from various mixing elements with filler concentration at 12 vol % are shown in Figure 9(a). The distributions are clearly bimodal or multimodal. The leftmost branch at about 1.8 μm and smaller may correspond to the unit particles and aggregates in the composites. The right part, where the distribution is greater than about 1.8 μm, may correspond to the agglomerates. It can be seen that the area fraction of the dispersed phase greater than 1.8 μm is smaller for the two dispersive elements indicating the efficient breakdown of the agglomerates while passing through the mixing section. The overall area fraction of the agglomerates Φ_a for d_i greater than 1.8 μm were calculated and listed in Table II for composites from various mixing elements. As expected, Φ_a from the two dispersive elements are smaller than that from the screw element.

The distribution curves of the area fraction of treated $CaCO_3$ filled composites from various mixing elements with filler concentration at 12 vol % are

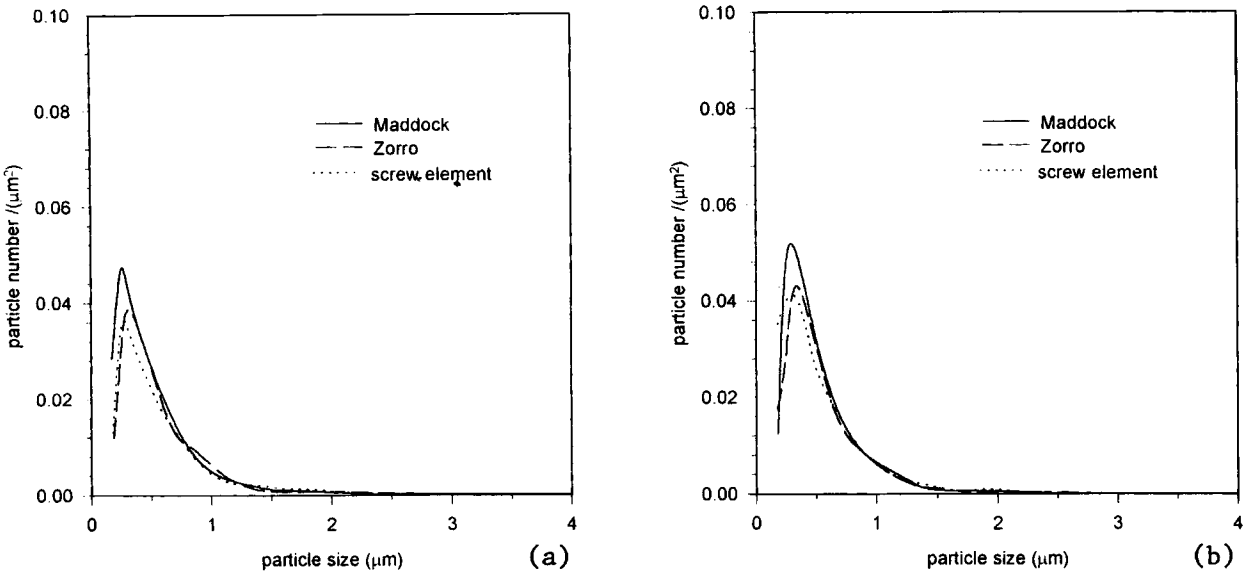

Figure 8 Particle size distribution of $CaCO_3$ filled composites from various mixing elements at 5 vol %: (a) without surface treatment and (b) with surface treatment.

shown in Figure 9(b). The distributions are also clearly bimodal or multimodal. The calculated Φ_a are listed in Table II. Apparently, the magnitudes of Φ_a of treated $CaCO_3$ are smaller than that of untreated particulates.

The distribution curves of the area fraction of the untreated and LICA12 treated $CaCO_3$ filled composites at 5 vol % from the three elements are shown in Figure 10(a,b). The shapes of these distribution curves are similar to that shown in Figure 9(a,b). They are all bimodal or multimodal distributions. Distribution greater than 1.8 μm corresponds to agglomerates; distribution smaller than 1.8 μm corresponds to unit particles and aggregates. The calculated Φ_a are listed in Table II. It can be seen that the magnitudes of Φ_a at 5 vol % are all smaller than their counterparts at 12 vol %, although the differences are not very great. The Φ_a at 20 vol % from the Maddock element are included for comparison. Once more they are the largest among all the samples under consideration. The effect of mixing at high filler concentration may be limited by the screw size

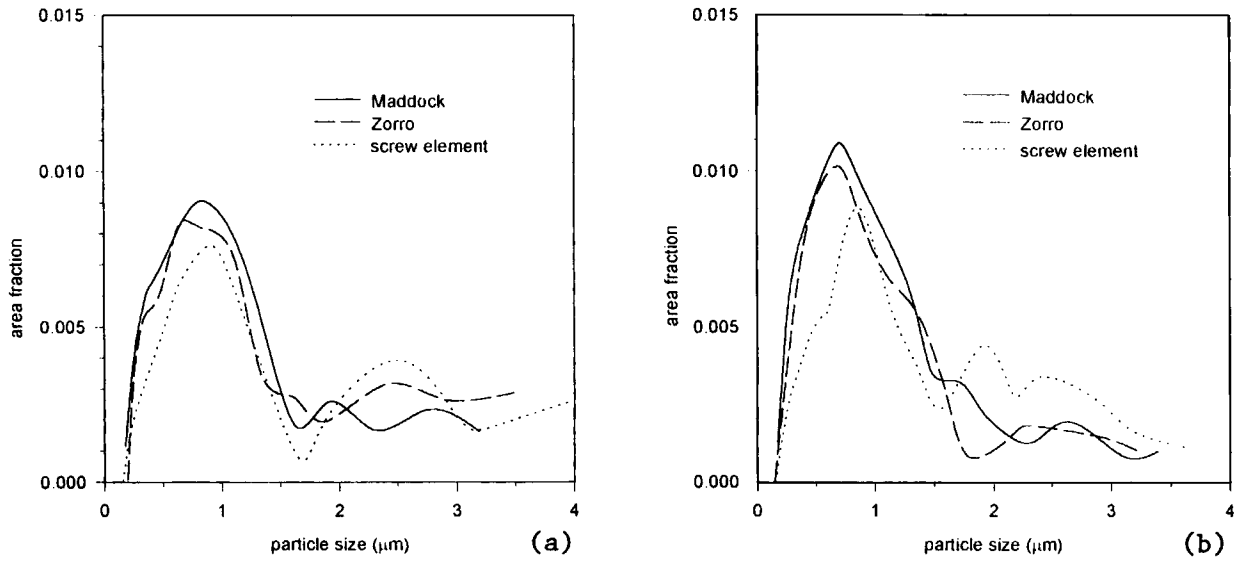

Figure 9 Area fraction distribution of $CaCO_3$ filled composites from various mixing elements at 12 vol %: (a) without surface treatment and (b) with surface treatment.

Table II Calculated ϕ_a for Specimens Compounded from Various Mixing Elements

Surface Treatment	Maddock	Zorro	Screw Element
Without			
5 vol %	0.00754	0.00970	0.01010
12 vol %	0.00953	0.01066	0.01543
20 vol %	0.04948		
With			
5 vol %	0.00511	0.00650	0.00845
12 vol %	0.00653	0.00834	0.0127
20 vol %	0.03815		

and the operation range of the laboratory scale extruder.

Notched Izod Impact Toughness

The plots of the notched Izod impact strength versus filler concentration of iPP/$CaCO_3$ composites with and without surface treatment from various mixing elements for a notch depth of 1 mm are shown in Figure 11(a,b). It can be seen that the impact strengths of the composites compounded from the Maddock and the Zorro elements are always higher than that from the screw element at the same filler concentration because of the low Φ_a of the composites from these dispersive elements. It can also be seen that the impact strengths are always higher for treated $CaCO_3$ filled composites whose Φ_a are also smaller than the untreated counterparts. It was shown that the extent of stress concentration around the inclusion in a matrix is proportional to the inclusion size. Large agglomerates of untreated $CaCO_3$ particles thus may initiate sample failure and lower the impact energy. Furthermore, failure initiation and propagation depends on the structure and properties of the composites. Structural inhomogeneities (aggregation, voids, etc.) favor initiation, while rigidity of the matrix promotes propagation. Very strong interactions between the untreated $CaCO_3$ particles and the matrix lead to a rigid interphase, resulting in decreased fracture resistance. However, weak interactions between the treated $CaCO_3$ particles and the matrix lead to dewetting and microvoid formation and enhance the impact toughness.[33,35]

The impact strengths of the composites also appear as functions of filler concentration. The strength increases with $CaCO_3$ content up to a maximum around 12 vol %; then it decreases. Such relation was also reported elsewhere.[29,34] The increase in toughness at low concentrations of the filler may be due to the local microplastic deformation arising from the microscopic cavities around the poorly bonded particles. The reduction in toughness at high filler concentrations is due to limited plastic flow of the PP matrix because the more ductile matrix is replaced by the more rigid dispersed particulates. The impact strength at 20 vol % is even lower than the virgin PP because of the inefficient compounding in the laboratory scale extruder at such high filler concentration.

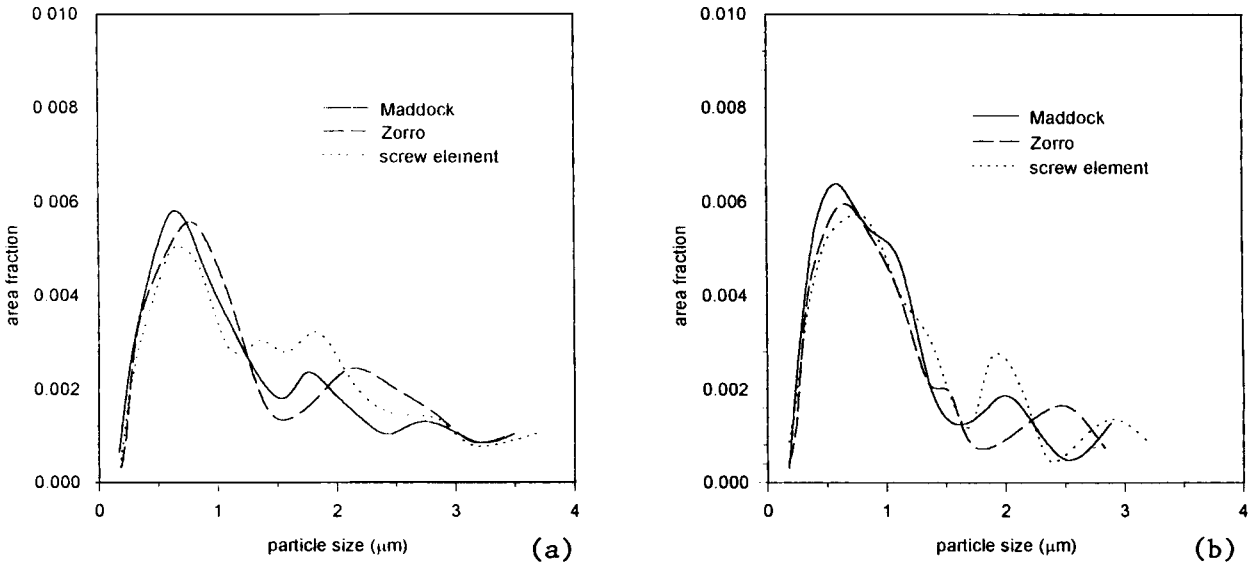

Figure 10 Area fraction distribution of $CaCO_3$ filled composites from various mixing elements at 5 vol %: (a) without surface treatment and (b) with surface treatment.

The notched impact strength was also measured for different notch depth, and therefore we were able to determine the fracture toughness G_c (Table III). The method proposed by Plati and Williams[36] was used to determine G_c by assuming linear elastic fracture behavior. The impact energy is related to the notch depth through the parameter ϕ, which is a function of the notch depth and the test geometry

$$J = J_k + G_c BD\phi \quad (2)$$

where J is the measured impact energy, J_k is the energy dissipated during impact as kinetic energy, and is determined by the intercept from the plot of J vs. $BD\phi$. ϕ is a geometrical factor defined as

$$\phi = C/[dC/d(a/D)] \quad (3)$$

and C is the compliance of the notched sample. ϕ was tabulated for Izod samples.[36] The values of ϕ were in the range 0.53–1.27 for our specimens.

The slope of the straight line of eq. (2) is G_c. However, this analysis assumes that the material under test shows linear elastic behavior and undergoes brittle fracture. Such brittle behavior may be confirmed from the SEM micrographs in Figures 3–6. Figure 12(a,b) show plots of J against $BD\phi$ for $CaCO_3$-filled composites with and without surface treatment. The filler concentrations are 12 vol %. We then plot relative G_c vs. filler concentration for composites from various mixing elements. Figure 13(a) is the plot of untreated $CaCO_3$-filled composites and figure 13(b) is the plot of LICA12 treated $CaCO_3$. The fracture toughness of the composites also appear as functions of filler concentration. Similarly, a maximum around 12 vol % can be seen in each curve in Figure 13(a,b). The toughness at 20 vol % is again lower than the virgin PP. It was suggested that the filler loading should be less than 20 vol % in order to increase the tensile and impact properties of $CaCO_3$-filled PP.[31] It can also be seen that the surface treatment improves the fracture toughness of the composites when comparing G_c values in Figure 13(b) with that in Figure 13(a). Furthermore, the G_c values for composites from the

Table III Fracture Toughness of G_c for Specimens Compounded from Various Mixing Elements

Surface Treatment	Maddock	Zorro	Screw Element
Without			
5 vol %	1.69	1.71	1.65
12 vol %	1.82	1.81	1.67
20 vol %	0.78	0.76	0.63
With			
5 vol %	1.80	1.83	1.72
12 vol %	2.13	2.0	1.82
20 vol %	0.91	0.83	0.72

Values in kilojoules per square meter.

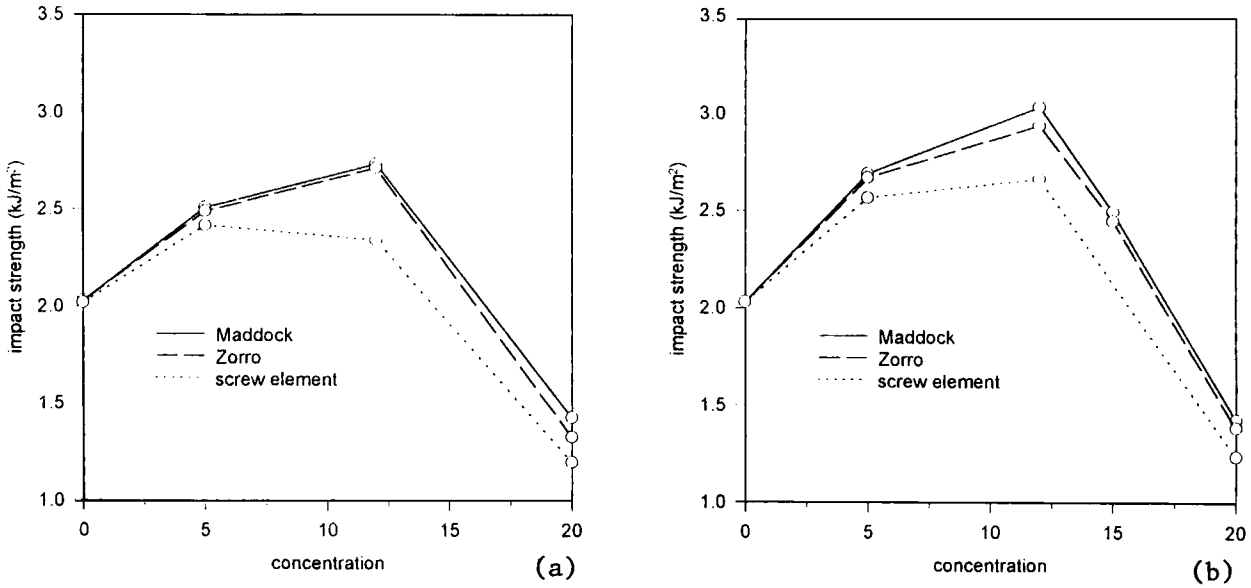

Figure 11 The notched impact strengths of the composites from various mixing elements: (a) without surface treatment and (b) with surface treatment. The notch depth is 1 mm.

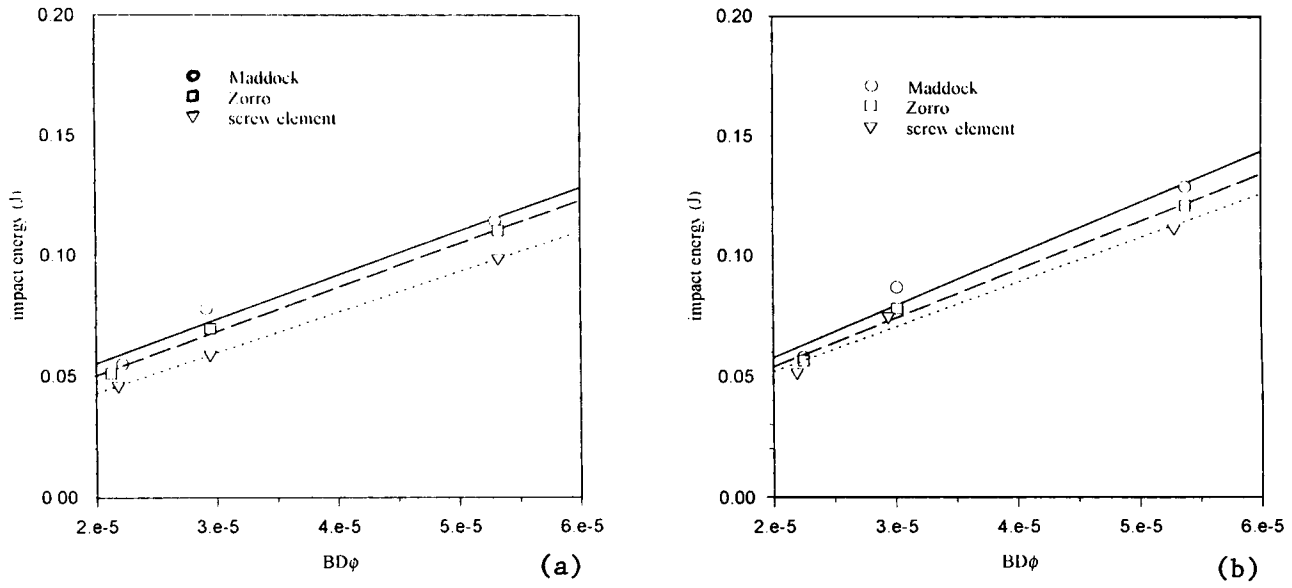

Figure 12 The impact energy J against $BD\phi$ for composites from various mixing elements: (a) without surface treatment and (b) with surface treatment. The filler loadings are 12 vol %.

screw element are generally lower than that from the Maddock and the Zorro mixing elements.

When G_c are plotted against Φ_a at different concentrations (Fig. 14), it can be clearly seen that for each concentration the G_c decreases as Φ_a increases. Note that the inclusions greater than about 1.8 μm were counted for calculating Φ_a. The samples with the same filler loading exhibit a pronounced decrease in toughness with the increasing value of Φ_a. It is worthy of note that the values of Φ_a for 12 and 5 vol % do not differ much. However, the fracture toughness has a significant increase in composites at the filler loading of 12 vol %. While large particles and agglomerates are detrimental to impact resistance of composites, the reinforcement of composites mainly arises from the incorporation of fine filler

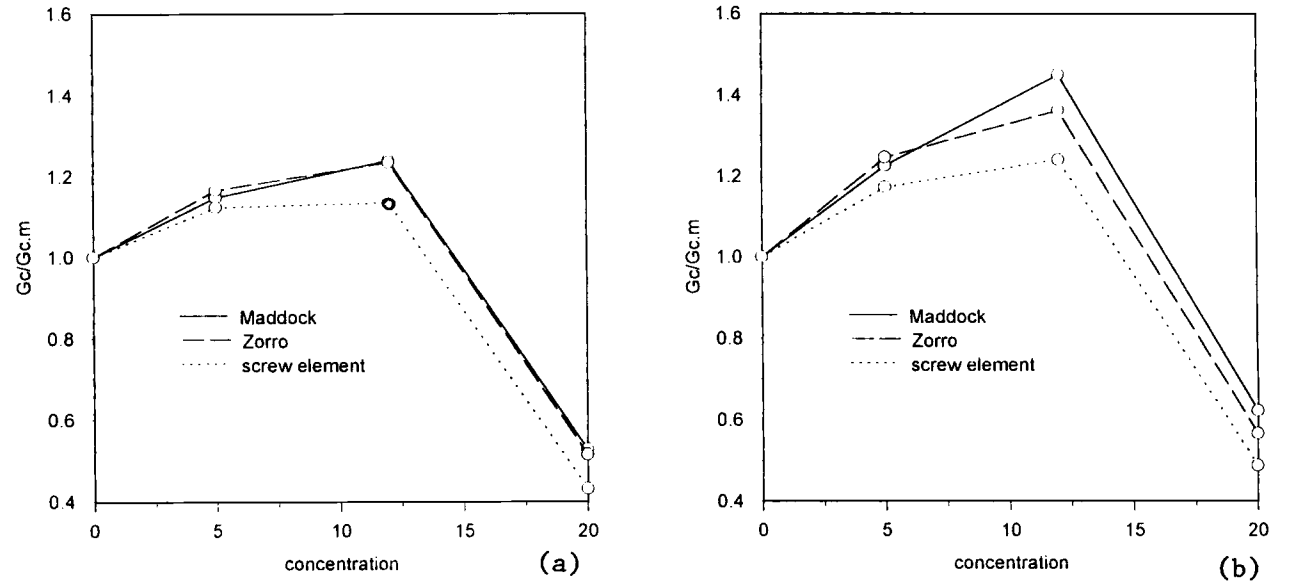

Figure 13 Fracture toughness vs. filler concentration for composites from various mixing elements: (a) without surface treatment and (b) with surface treatment.

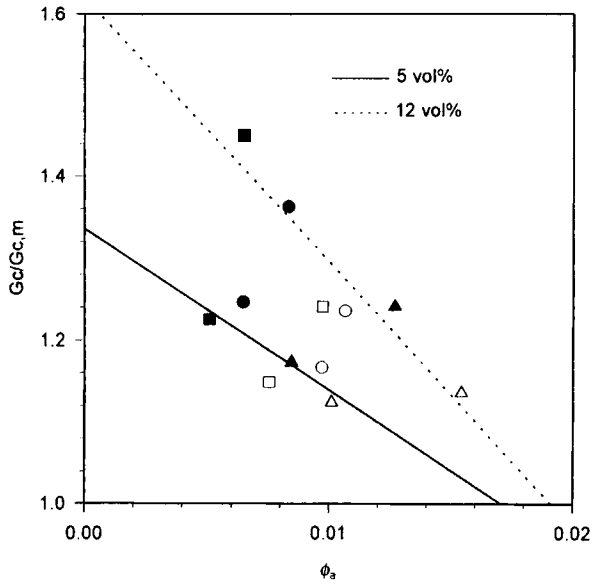

Figure 14 Fracture toughness vs. Φ_a at various filler concentrations.

particles. Thus it is expected that the marked increase in G_c at 12 vol % is due to the high concentration of fine particles. We used the composites filled with treated $CaCO_3$ compounded from the Maddock element as examples. We calculated the overall area fraction of unit particles and aggregates with particle size less than 1.8 μm. It was found that the calculated values were 0.057 and 0.028 for filler loadings of 12 and 5 vol %, respectively. Therefore, to attain the increased composite toughness with regard to the parent matrix, it was necessary to use filler with fine particles of about 1 μm to ensure its good dispersion. However, the sensitivity toward agglomerates and large particles of the filler may vary with different polymer matrix and filler concentration.

CONCLUSION

It follows from the presented results that in the composites with the same filler loading the measurement of content of inhomogeneities greater than about 1.8 μm represents a reliable and sensitive method for the correlation of fracture toughness in the system of PP–calcium carbonate.

The area fraction of agglomerates is much lower for composites compounded from the dispersive mixing elements, i.e., the Maddock and the Zorro elements. Both the impact strength and the fracture toughness increases as the overall area fraction of agglomerates and large particles decreases. This may be ascribed to a large amount of uneven voids and defects around the interfaces between agglomerates (or large particles) and the matrix. On the other hand, the effective dispersion of fine filler particles is responsible for the reinforcement of the composites.

This study clearly demonstrates that incorporation of treated $CaCO_3$ fillers greatly modifies the impact strength of PP, but only at a moderate loading of filler. SEM micrographs with image analysis reveal better dispersion and decreased agglomeration of filler particles upon treatment of LICA12, which is well known as an effective coupling agent. Furthermore, proper choice of a mixing device plus effective surface treatment would give rise to the maximum improvement.

The financial support of this research by the National Science Council of Taiwan, Republic of China, under Grant NSC-82-0405-029-002 is gratefully acknowledged.

REFERENCES

1. L. E. Nielsen, *Mechanical Properties of Polymers and Composites,* Marcel Dekker, New York, 1974, p. 380.
2. L. Nicolasis and R. A. Mashelker, *J. Appl. Polym. Sci.,* **20,** 561 (1976).
3. M. Sumita, T. Ookuma, K. Miyasaka, and K. Ishikawa, *J. Appl. Polym. Sci.,* **27,** 3039 (1982).
4. M. Sumita, T. Shizuma, K. Miyasaka, and K. Ishikawa, *J. Macromol. Sci. Phys.,* **B22,** 601 (1983).
5. V. P. Chacko, R. J. Farris, and F. E. Karasz, *J. Appl. Polym. Sci.,* **28,** 2701 (1983).
6. S.-R. Dai and M. R. Piggott, *Polym. Comp.,* **7,** 19 (1986).
7. G. Levita, A. Marchetti, and A. Lazzeri, *Polym. Comp.,* **10,** 39 (1989).
8. I. Sasaki, K. Ito, T. Kodama, and F. Ide, *Kobunshi Ronbunshu,* **33,** 162 (1976).
9. T. Nakatuka, H. Kawasaki, and K. Itadani, *J. Colloid Interface Sci.,* **82,** 298 (1981).
10. Y. N. Sharma, R. D. Patel, I. H. Dhimmar, and I. S. Bhardwai, *J. Appl. Polym. Sci.,* **27,** 97 (1982).
11. K. Mitsuishi, S. Kodama, and H. Kawasaki, *Polym. Eng. Sci.,* **25,** 1069 (1985).
12. K. Mitsuishi, S. Kodama, and H. Kawasaki, *Kobunshi Ronbunshu,* **43,** 43 (1986).
13. J. W. Ess, P. R. Hornsby, S. Y. Yin, and M. J. Bevis, *Plast. Rubber Proc. Appl.,* **4,** 7 (1984).
14. A. M. Riley, C. D. Paynter, P. M. McGenity, and J. M. Adams, *Rubber Proc. Appl.,* **14,** 85 (1990).
15. S. F. Xavier, J. M. Schultz, and K. Friedrich, *J. Mater. Sci.,* **25,** 241 (1990).

16. C. Rauwendaal, in *Mixing in Polymer Processing*, C. Rauwendaal Ed., Marcel Dekker, New York, 1991, p. 160.
17. C. H. Leigh-Dagmore, *Rubber Chem. Technol.*, **29**, 1303 (1956).
18. N. A. Stamp and H. E. Railsback, *Rubber World*, **151**, 41 (1964).
19. B. B. Boonstra and A. I. Medalia, *Rubber Age*, **92**, 892 (1963).
20. E. M. Dannenberg, *Ind. Eng. Chem.*, **44**, 813 (1952).
21. K. Min and J. L. White, *Rubber Chem. Technol.*, **60**, 361 (1987).
22. R. F. Cembrola, *Rubber Chem. Technol.*, **56**, 233 (1983).
23. B. B. Boonstra and A. I. Medalia, *Rubber Chem. Technol.*, **36**, 15 (1963).
24. A. V. Galanti and L. Sperling, *J. Appl. Polym. Sci.*, **14**, 2785 (1970).
25. Y. Suetsugu, J. L. White, and T. Kyu, *Adv. Polym. Technol.*, **7**, 427 (1987).
26. Y. Suetsugu, T. Kikutani, T. Kyu, and J. L. White, *Colloid Polym. Sci.*, **268**, 118 (1990).
27. Y. Suetsugu, *Int. Polym. Processing*, **5**, 184 (1990).
28. P. Bajaj, N. K. Jha, and R. K. Jha, *Polym. Eng. Sci.*, **29**, 557 (1989).
29. S. N. Maiti and P. K. Mahapatro, *J. Appl. Polym. Sci.*, **42**, 3101 (1991).
30. M. Bramuzzo, A. Savadori, and D. Bacci, *Polym. Comp.*, **8**, 1 (1985).
31. E. Nezbedova, J. Ponesicky, and M. Sova, *Acta Polym.*, **41**, 36 (1990).
32. S. Miyata, T. Imahashi, and H. Auabuki, *J. Appl. Polym. Sci.*, **25**, 415 (1980).
33. J. Jancar and J. Kucera, *Polym. Eng. Sci.*, **30**, 707 (1990).
34. V. Svehlova and E. Poloucek, *Angew. Makromol. Chem.*, **153**, 197 (1987).
35. B. Pukanszky, *New Polymeric Mater.*, **3**, 205 (1992).
36. E. Plati and J. G. Williams, *Polym. Eng. Sci.*, **15**, 470 (1975).

Received July 7, 1995
Accepted October 30, 1995